CHALMERS

Road Vehicle Aerodynamics Advanced

CFD Project: Vera

TEDDY HOBEIKA & JOHAN ZAYA

10/23/2011

Summary

This report is a part of the advanced course of Road Vehicle Aerodynamics and is the final examination of a project with focus on Computational Fluid Dynamics and the use of the software used for simulating the aerodynamics of a vehicle. The Vehicle in focus in this is Vera, which a vehicle built to compete in the Shell EcoMarathon where the aim is to travel the longest distance possible with one liter of fuel. The aim of the project is to gain knowledge and experience of the CFD tools, investigate the aerodynamics of Vera to see what is good and what can be improved. The results from the investigations are then implemented in the design of a new vehicle for the competition, the Vera 2.

CFD results are highly dependent on the mesh and solving setting so all setting should be carefully chosen. Running in a couple solving scheme and 2nd order upwind discretization has proven to give the most accurate results in the simulations. For chosing the turbulence model, the application and the y_plus values have to be taken into consideration. Down force/lift is not as sensitive to ground clearance and pitching the vehicle as it is to the shape of the front wheelcovers that are creating a Venturi effect on Vera resulting in downforce.

Introduction

The area of aerodynamics is a vital part of vehicle design where the performance can be enhanced if carefully planned out. Vehicle handling, cooling and fuel consumption are examples where aerodynamics has a huge effect. In this report, the focus is on a vehicle designed and built for the Shell Eco Marathon competition where the aim is to travel the longest distance possible on one liter of fuel. The vehicle is called Vera and is a part of the Chalmers Eco Marathon team and is in the prototype vehicle class. Vera is a three wheel vehicle with a small combustion engine, front wheel steering and a light weight carbon fiber body with a tear drop resembling aerodynamic design. As stated, the idea of the competition is to keep down fuel consumption, therefore the importance of weight and aerodynamics is crucial. The weight of Vera is around 30 kg, which is seen as a competitive number regarding other competition vehicles. However the body shape regarding aerodynamics isn’t considered to be as competitive, even though given a tear drop shape which is seen as the optimal shape for drag reduction. The aim of this project is to investigate the aerodynamic forces on Vera and how they can be reduced and then further on implement the gained knowledge on designing Vera 2 which will be the new vehicle for the Chalmers Eco Marathon team.

The investigations are carried out using Computational Fluid Dynamics (CFD) software’s which numerically solves equations governing the flow, i.e. Navier Stokes equations. The software’s encountered are Ansa, Fluent and Paraview. The CAD-cleaning of the model is done in Ansa and so is the surface and volume mesh. The model is then solved in Fluent and post processed in Paraview. CFD software’s are great tools for aerodynamics investigations and can give sufficient accurate results that can be implemented in the design.

The project is carried out by running simulations on the original design of Vera versus three other configurations with changes on the area’s that are considered to be most effective. The original Vera is shown in figure XX and the configurations in figure XX. Further on, investigations on different types of mesh and solving setting are carried out in order to gain a more in-depth understanding of the software’s and results. Config B is morphed in the front by 200 mm, C is raised by 15 mm and D is tilted -0.5 degrees. All configs are meshed with a fine mesh, but a it is also compared with a less fine mesh which is referred to as congfig E. The results and knowledge is then implemented on the first version of Vera 2 which is also covered within this report. The final version of Vera 2 will be a result of several configurations and many iterations which will be documented in a later report.

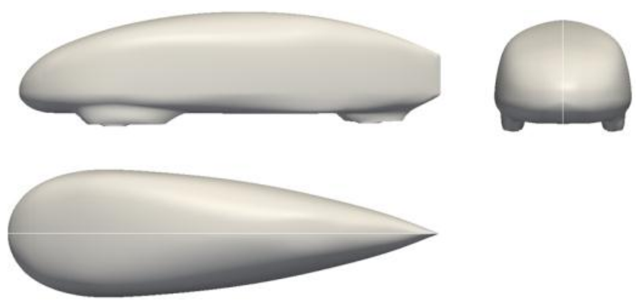

Figure 1. Vera

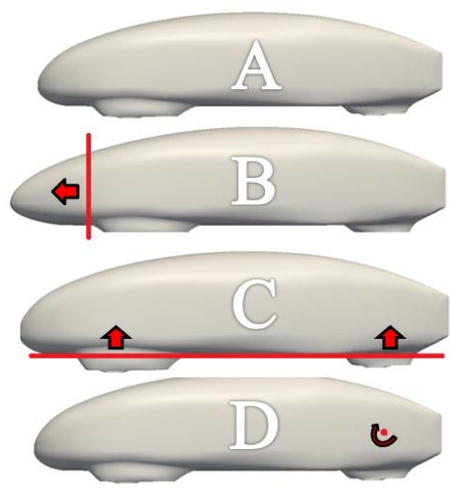

Figure 2. Configuration setup

Theory

Computational Fluid Dynamics (CFD) is the use of numerical methods and algorithms to simulate the flow around or through a body. All flows can be described using three equations:

- Continuity : $\frac{\partial \rho}{\partial t} + \frac{\partial \rho u_i}{\partial x_i} = 0$
- Conservation of momentum equation: $\frac{\partial \rho u_i}{\partial t} + \frac{\partial \rho u_i u_j}{\partial x_j} = -\frac{\partial p}{\partial x_i} + \frac{\partial \tau_{ij}}{\partial x_j} + \rho f_i$
- Conservation of energy equation: $\frac{\partial \rho E}{\partial t} + \frac{\partial \rho u_j E}{\partial x_j} = \rho q + \frac{\partial}{\partial x_j}\left(k \frac{\partial T}{\partial x_j}\right) - \frac{\partial u_j p}{\partial x_j} + \frac{\partial u_i \tau_{ij}}{\partial x_j} + \rho f_i u_i$

Assuming that the flow is incompressible and the temperature is constant then there is no need to solve the energy equation and both the continuity and momentum equations can be simplified to the following two equations:

$$\frac{\partial u_i}{\partial x_i} = 0 \quad ; \quad \rho \frac{\partial u_i u_j}{\partial x_j} = -\frac{\partial p}{\partial x_i} + \frac{\partial \tau_{ij}}{\partial x_j} + \rho f_i$$

where $p = \rho RT$

If Reynolds Averaged Navier Stokes (RANS) variables are substituted into the equation then it beco

$$\frac{\partial \bar{U}_i}{\partial x_i} = 0 \quad ; \quad \rho \bar{U}_j \frac{\partial \bar{U}_i}{\partial x_j} = -\frac{\partial \bar{P}}{\partial x_i} + \frac{\partial}{\partial x_j}\left(\mu \frac{\partial \bar{U}_i}{\partial x_j} - \rho \overline{u_i u_j}\right)$$

The k-epsilon model introduces a turbulent viscosity factor (eddy viscosity) which can be written as $\mu_t = \rho C_\mu \frac{k^2}{\varepsilon}$

For a standard model the factor C_μ is set to 0.09 however it is calculated in the realizable model.

The k-epsilon has two main equations which are the turbulent kinetic energy and the dissipation equations given by Pope as:

$$\frac{\partial k}{\partial t} + \bar{U}_i \frac{\partial k}{\partial x_i} = \frac{\partial}{\partial x_i}\left(\frac{\nu_t}{\sigma_k}\frac{\partial k}{\partial x_i}\right) + \nu_t \left(\frac{\partial \bar{U}_i}{\partial x_j} + \frac{\partial \bar{U}_j}{\partial x_i}\right)\frac{\partial \bar{U}_i}{\partial x_j} - \varepsilon$$

$$\frac{\partial \varepsilon}{\partial t} + \bar{U}_i \frac{\partial \varepsilon}{\partial x_i} = C_{\varepsilon 1}\sqrt{S_{ij}S_{ij}}\varepsilon - C_{\varepsilon 2}\frac{\varepsilon^2}{k + \sqrt{\nu\varepsilon}} + \frac{\partial}{\partial x_i}\left(\left(\nu + \frac{\nu_t}{\sigma_\varepsilon}\right)\frac{\partial \varepsilon}{\partial x_i}\right)$$

Case Setup

In the following section, the setting for the cases are shown and discussed. The software's contains numerous numbers of different setups and configurations, and to conclude which ones are best is not easy. All of the different setups are not investigated, however the ones that were used are considered to be suitable for the desired results.

Surface and Volume Mesh settings:

The setting for the mesh is the same for all configurations. The surface mesh on the vehicle is between 2.5 to 5 mm. On the tail and the wheel covers the mesh is 2.5 mm followed by 5 mm around the whole body. The mesh on the wind tunnel is up to 400 mm and within there are 4 refinement boxes. The size box for the whole has a mesh 20 mm, followed by boxes with a finer mesh of 10 mm for the underbody, the rear and the nose. Figure 3 shows the size boxes. The box for the whole vehicle has a bigger area behind the vehicle in order to get a good illustration of the flow and the losses. In this case there is no wake behind the vehicle since it of tear drop design, however very important for regular vehicles where a wake is certain and needs to be illustrated accurately. On the underbody, the mesh is very fine since the ground clearance is very small and likewise the area of the wheel covers, therefore building up big cell sizes will not give a good representation of the flow. The same for the nose and the rear cell sizes. The boundary layers are built around the vehicle, there are five with a thickness of 0.2 mm. To gain better understanding of the refining of the mesh and its effect on results, a configuration with a less fine size boxes is simulated. The differences between the meshes can be seen in figure 4. The quality of the mesh is considered to be quite good, where no elements are on the surface and no more than a hundred elements of in the volume mesh, not affecting the area near the vehicle. The total number of cells for all configurations varies between 5.5 to 5.8 million cells.

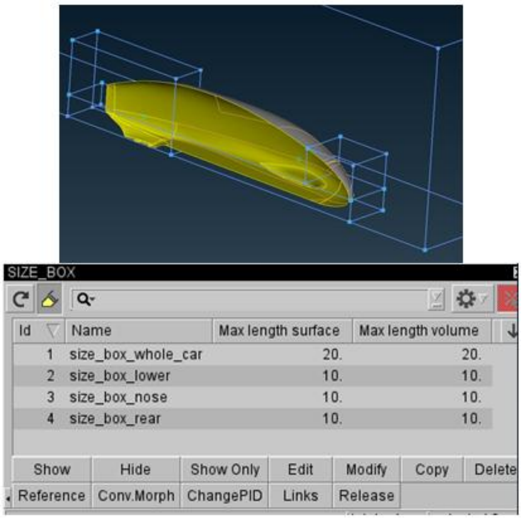

Figure 3. Size boxes

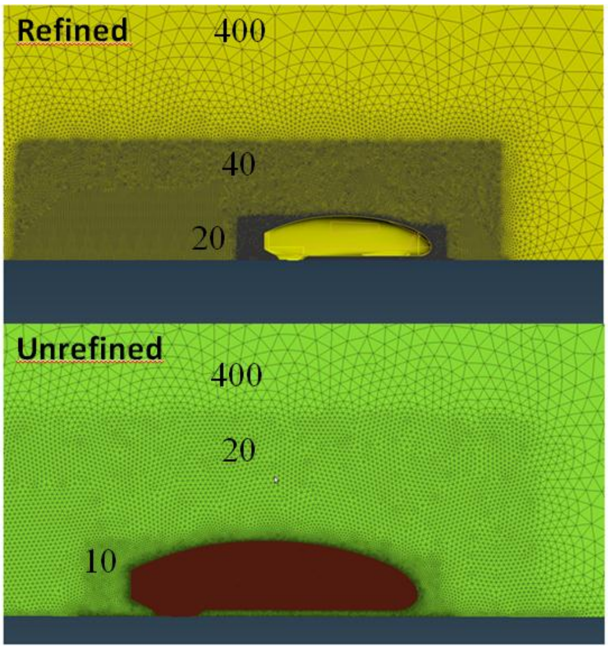

Figure 4 Refine vs. Unrefined cell sizes

PID division:

The division of the PID's can be seen in the figures below.

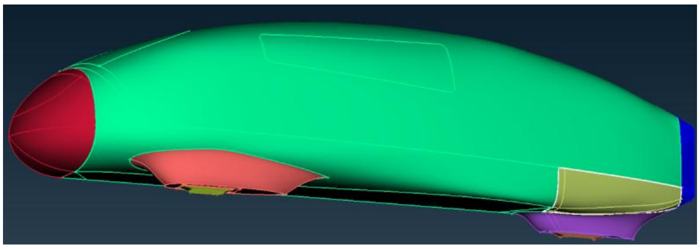

Figure 5. PID division

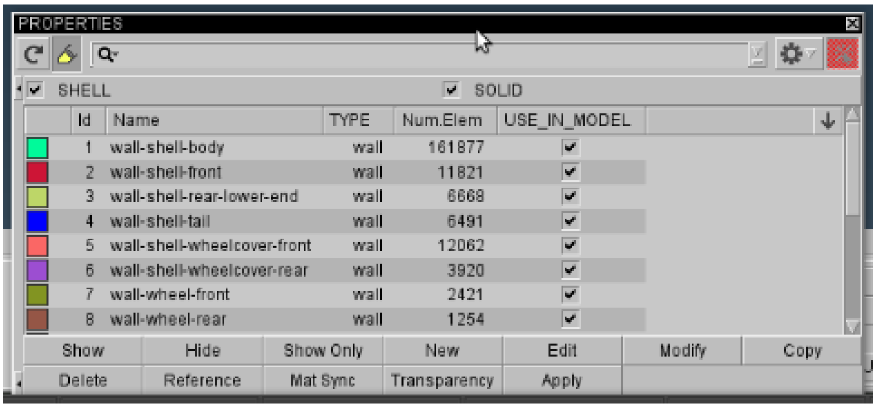

PROPERTIES

SHELL   SOLID

Id	Name	TYPE	Num.Elem	USE_IN_MODEL
1	wall-shell-body	wall	161877	✔
2	wall-shell-front	wall	11821	✔
3	wall-shell-rear-lower-end	wall	6668	✔
4	wall-shell-tail	wall	6491	✔
5	wall-shell-wheelcover-front	wall	12062	✔
6	wall-shell-wheelcover-rear	wall	3920	✔
7	wall-wheel-front	wall	2421	✔
8	wall-wheel-rear	wall	1254	✔

Figure 6 PID division setup

Solving settings:

The turbulence model used is k-epsilon realizable and upwind second order discretization. Turbulent intensity is set to 0.1 and viscosity ration to 200. Coupled solving scheme is used, however also simple is used to see what difference's it gives. Standard wall boundary conditions were used. For the convergence, Courant number is 20 and the under-relaxation factor is set to 0.3 for both momentum and pressure. The boundary conditions are moving ground and rotating wheels. Velocity inlet is set to 8 m/s and outlet set to pressure outlet.

Results and discussion

The results will now be presented in order where all configurations are compared to are compared to the original Vera reference vehicle.

Case A

Residuals

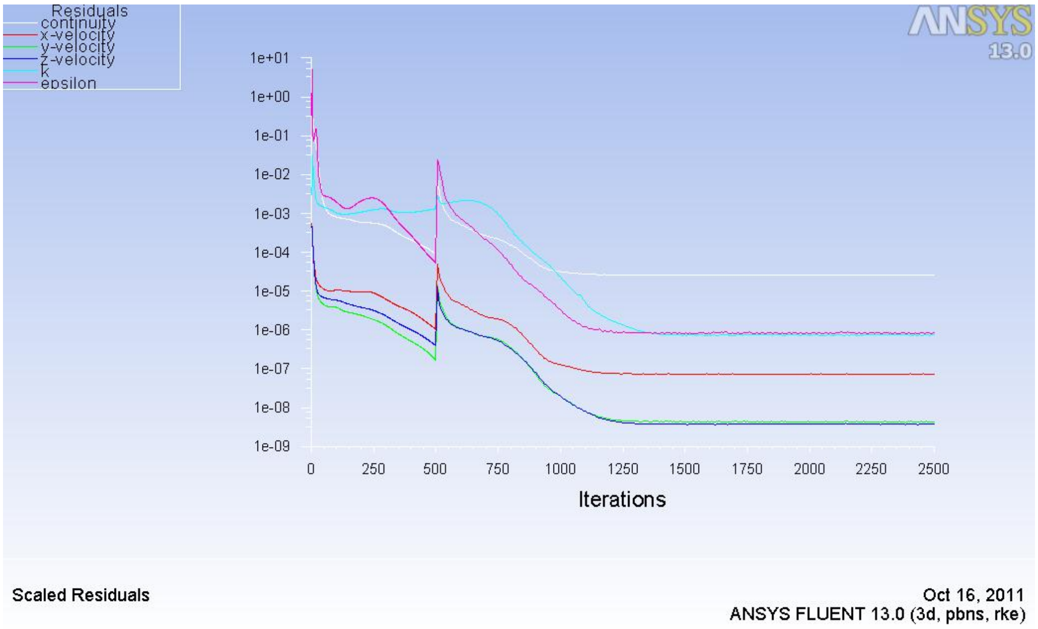

Plot 1. Residuals plot for case A

Aerodynamic forces

	Force x-dir (N)	Cd*A	Cd	%	Force z-dir (N)	Cl*A	Cl
Shell-body	-0.43	-0.010	-0.028	-27.9%	2.85	0.068	0.184
Shell-front	2.07	0.049	0.134	132.8%	-0.77	-0.018	-0.050
Wheel front	-0.01	0.000	0.000	-0.3%	-0.24	-0.006	-0.016
Wheel rear	0.00	0.000	0.000	-0.3%	-0.04	-0.001	-0.002
wheelcover-front	0.02	0.000	0.001	1.3%	-3.05	-0.073	-0.197
wheelcover-rear	-0.01	0.000	0.000	-0.5%	-0.22	-0.005	-0.015
rear-lower	0.01	0.000	0.001	0.9%	-0.23	-0.006	-0.015
tail	-0.09	-0.002	-0.006	-6.0%	0.00	0.000	0.000
Miscellaneous	0.00	0.000	0.000		0.00	0.000	0.000
TOTAL	1.556	0.037	0.101	100%	-1.704	-0.041	-0.110

Table 1. Distribution of aerodynamic forces and coefficients for Case A

Discussion

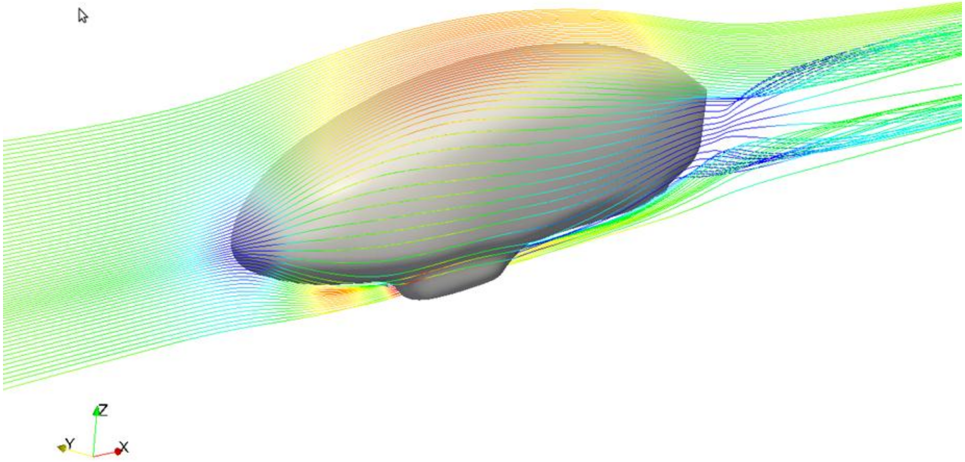

Figure 7. Stream lines around Vera for Case A

As shown in Figure 7 the flow around Vera is really smooth along the body since it has been designed to have a “tear-drop shape’’, thus no large vortices are generated behind Vera and no rear wake formation is present although of course the flow behind it is slower than the free stream flow due to energy losses.

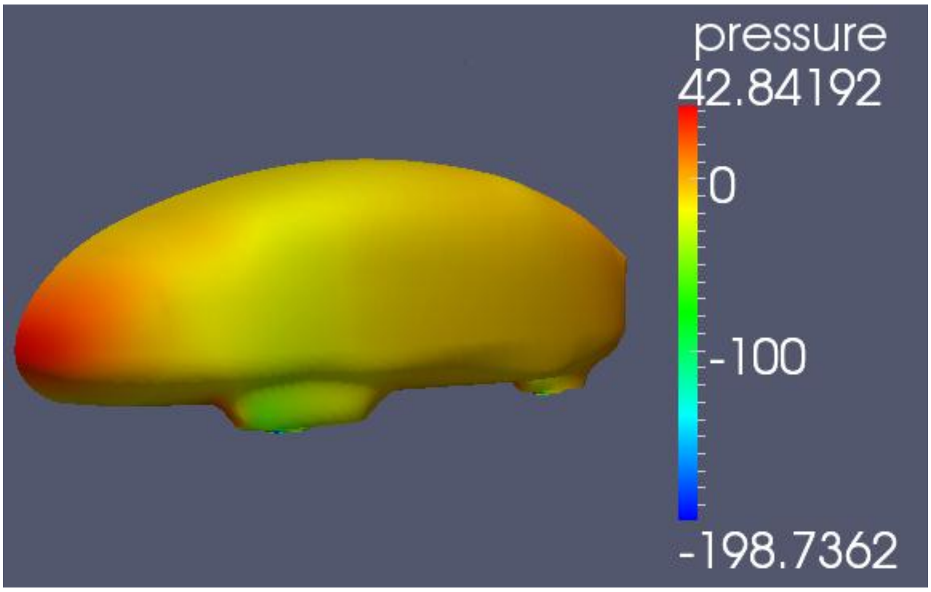

Figure 8. Pressure distribution on Vera in Case A

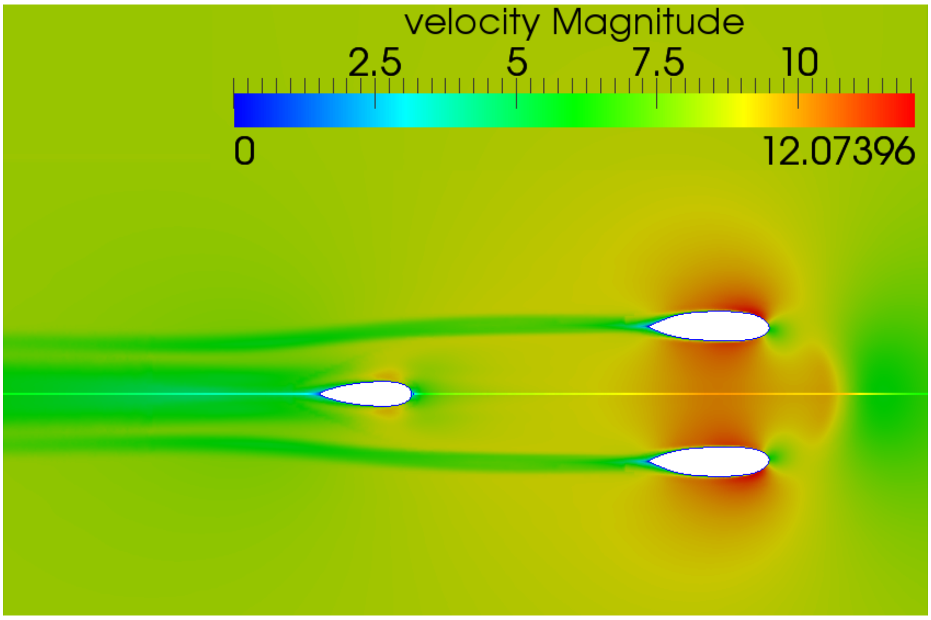

Figure 9. Flow velocity 35mm above ground for Case A

As shown above in Figure 8 there is a big stagnation pressure on the front nose of Vera due to the large nose radius this results in a 134 counts contribution to the total drag. Then the pressure along the body is more or less uniformly distributed except for some low pressure regions around the front wheelcover. From Figure 9 we can also notice that the flow accelerated in between the front wheelcovers which results in a low pressure region thus giving downforce. This phenomena is can be recognized as the Venturi effect This can also be seen in Table one where the lift contribution from the front wheel covers is -197 counts.

Case B

Residuals

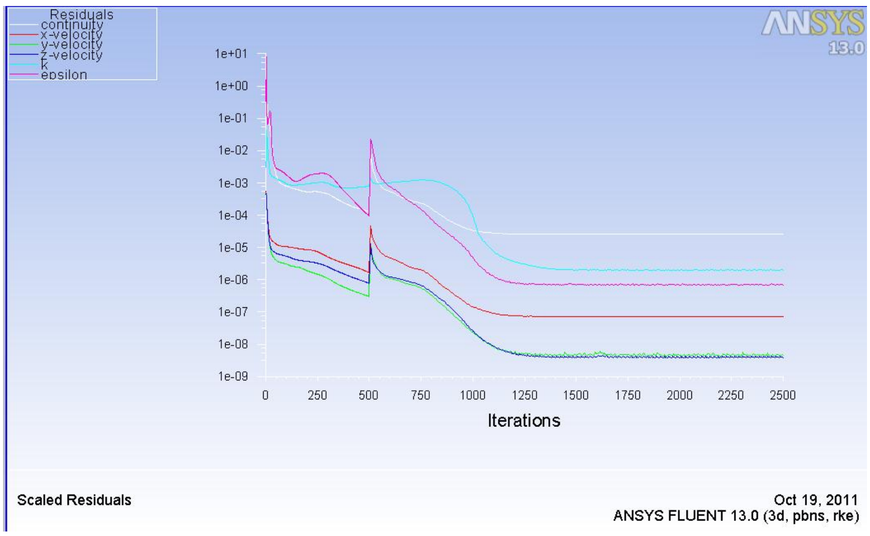

Plot 2. . Residuals plot for case B

Aerodynamic forces

	Force x-dir (N)	Cd*A	Cd	%	Force z-dir (N)	Cl*A	Cl
Shell-body	0.07	0.002	0.005	4.5%	1.68	0.040	0.109
Shell-front	1.52	0.036	0.098	97.5%	-0.58	-0.014	-0.037
Wheel front	0.00	0.000	0.000	0.2%	-0.22	-0.005	-0.014
Wheel rear	0.00	0.000	0.000	-0.3%	-0.03	-0.001	-0.002
wheelcover-front	0.07	0.002	0.004	4.3%	-2.93	-0.070	-0.189
wheelcover-rear	-0.01	0.000	-0.001	-0.7%	-0.19	-0.005	-0.012
rear-lower	0.01	0.000	0.001	0.6%	-0.20	-0.005	-0.013
tail	-0.10	-0.002	-0.006	-6.2%	0.00	0.000	0.000
Miscellaneous	0.00	0.000	0.000		0.00	0.000	0.000
TOTAL	1.563	0.037	0.101	100%	-2.467	-0.059	-0.159

Table 2. Distribution of aerodynamic forces and coefficients for Case B

	ΔCd	ΔCl
Shell-body	0.033	-0.076
Shell-front	-0.035	0.013
Wheel front	0.001	0.001
Wheel rear	0.000	0.000
wheelcover-front	0.003	0.008
wheelcover-rear	0.000	0.002
rear-lower	0.000	0.002
tail	0.000	0.000
TOTAL	0.000	-0.049

Table 3. Drag and lift differences over the PIDs and total comparing Case B to Case A

Discussion

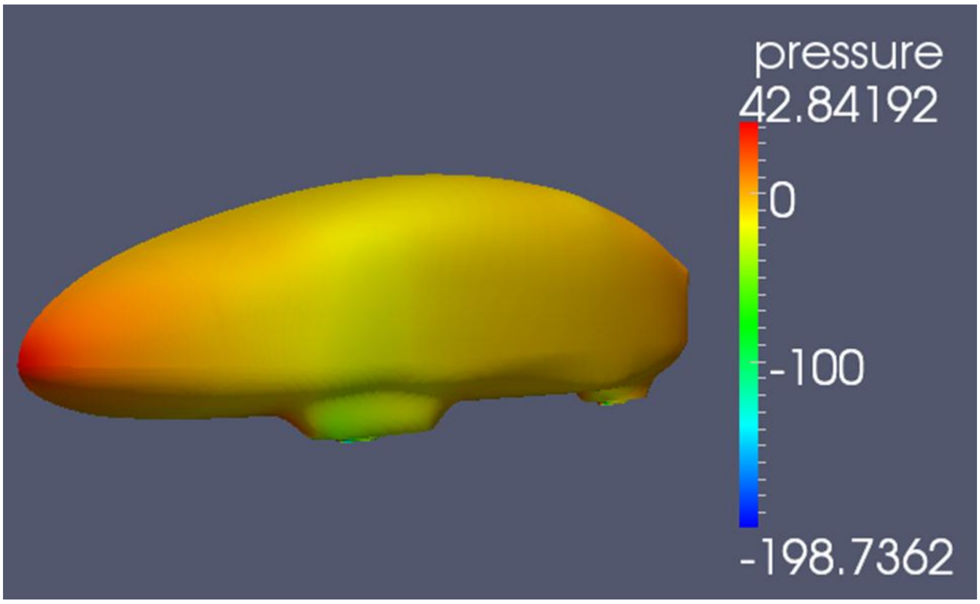

Figure 9. Pressure distribution on Vera in Case B

As shown in figure 9 and Table3, the area of stagnation pressure on the nose has been reduced thus resulting in a decrease of 35 drag counts. However one can also see that the pressure along the vehicle body increased thus resulting in an increase of 33 drag counts. So the total drag was not affected by the changes.

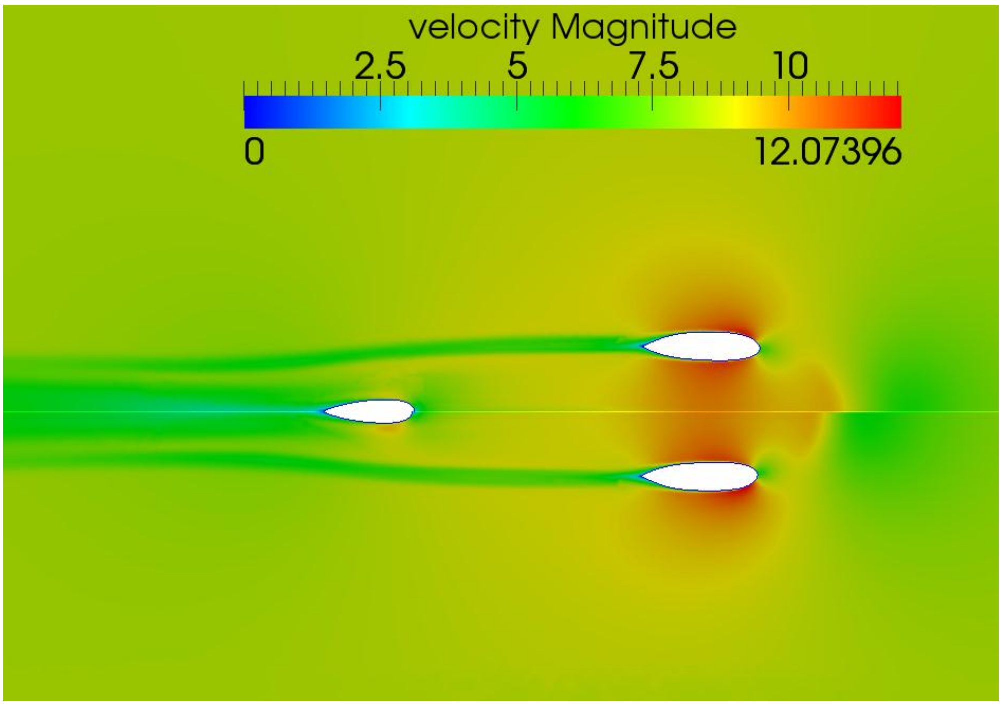

Figure 10. . Flow velocity 35mm above ground for Case A(lower half) and Case B(upper half)

As shown in figure 10, the morphed nose still resulted in the same acceleration of flow between the wheels. It also actually accelerated the flow over a longer area since the nose was 200mm longer. So since the low pressure region is now bigger, then it covers more surface area on Vera thus resulting in an increase in downforce by 49 counts.

Case C

Residuals

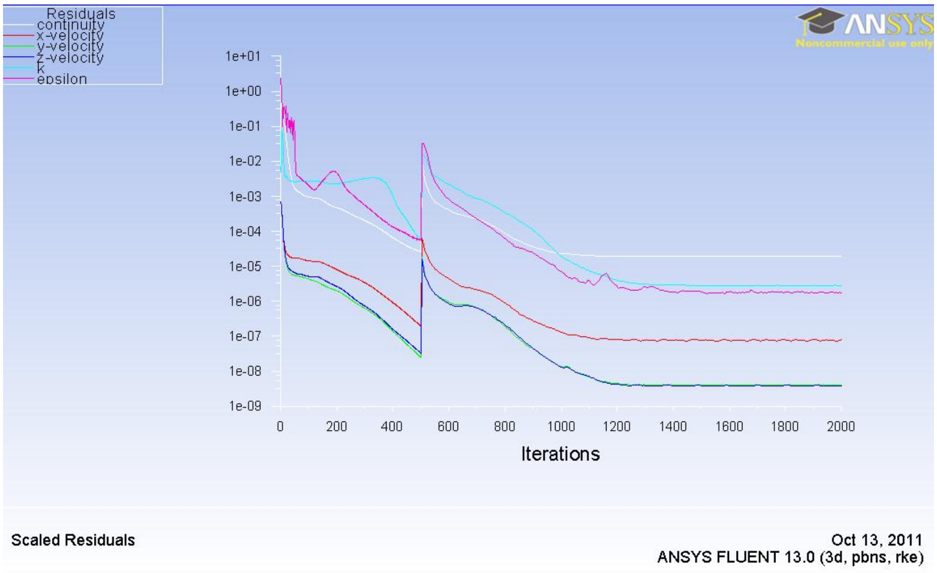

Plot 3. Residuals plot for case C

- *Aerodynamic forces*

	Force x-dir (N)	Cd*A	Cd	%	Force z-dir (N)	Cl*A	Cl
Shell-body	-0.42	-0.010	-0.027	-26.2%	3.07	0.073	0.196
Shell-front	2.04	0.049	0.130	128.1%	-0.88	-0.021	-0.056
Wheel front	0.00	0.000	0.000	-0.2%	-0.24	-0.006	-0.016
Wheel rear	0.00	0.000	0.000	-0.3%	-0.05	-0.001	-0.003
wheelcover-front	0.05	0.001	0.003	3.0%	-3.01	-0.072	-0.192
wheelcover-rear	0.00	0.000	0.000	-0.2%	-0.26	-0.006	-0.017
rear-lower	0.03	0.001	0.002	1.7%	-0.27	-0.006	-0.017
tail	-0.09	-0.002	-0.006	-5.8%	0.00	0.000	0.000
Miscellaneous	0.00	0.000	0.000		0.00	0.000	0.000
TOTAL	1.593	0.038	0.102	100%	-1.643	-0.039	-0.105

Table 4. Distribution of aerodynamic forces and coefficients for Case C

	ΔCd	ΔCl
Shell-body	0.001	0.012
Shell-front	-0.003	-0.006
Wheel front	0.000	0.000
Wheel rear	0.000	0.000
wheelcover-front	0.002	0.005
wheelcover-rear	0.000	-0.002
rear-lower	0.001	-0.002
tail	0.000	0.000
TOTAL	0.001	0.005

Table 5. Drag and lift differences over the PIDs and total comparing Case C to Case A

Discussion

In Case C, Vera was raised by 15mm which makes the total ground clearance to be around 80 mm instead of 65mm. This had no significant effect on drag and a decrease of 5 counts of downforce. This usually is pretty close to the uncertainty of CFD simulations, however since all values were converging to plus or minus zero counts for both drag and lift, and since sometimes the same mesh has been run two times and produced identical results within plus or minus one count then we can actually say that raising the vehicle will actually decrease downforce slightly however the accuracy of predicting that decrease is highly dependent on the mesh size which in our case could not be less than 10 mm not to increase mesh size. So the mesh might not have been fine enough to accurately detect the changes in geometry fo such small changes.

Case D

Residuals

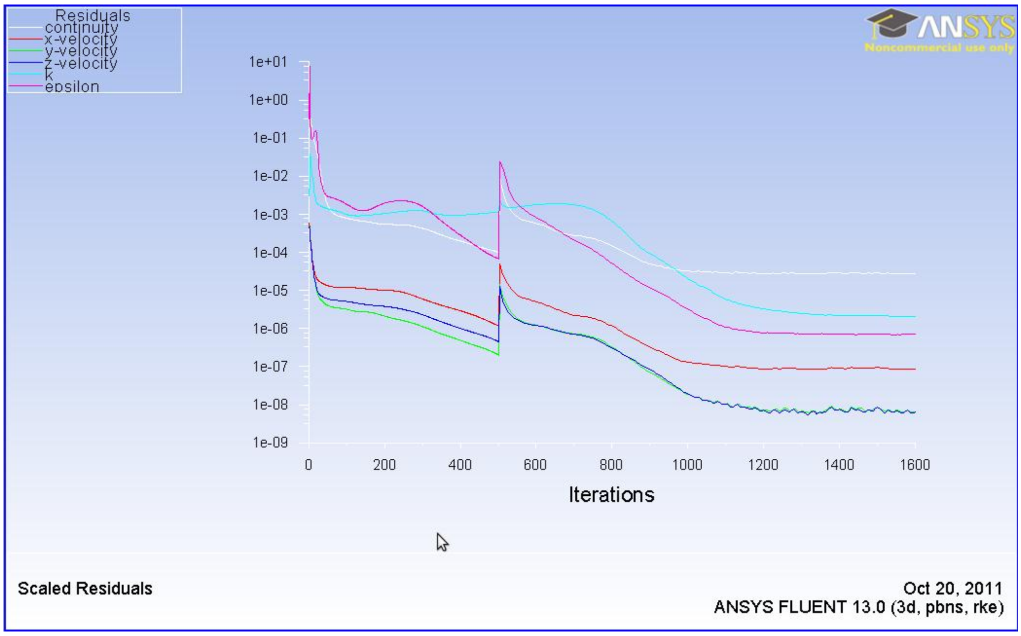

Plot 4. Residuals plot for case D

Aerodynamic forces

	Force x-dir (N)	Cd*A	Cd	%	Force z-dir (N)	Cl*A	Cl
Shell-body	-0.40	-0.010	-0.026	-25.5%	3.50	0.084	0.223
Shell-front	2.05	0.049	0.131	129.5%	-0.72	-0.017	-0.046
Wheel front	-0.01	0.000	0.000	-0.5%	-0.25	-0.006	-0.016
Wheel rear	-0.01	0.000	0.000	-0.3%	-0.04	-0.001	-0.003
wheelcover-front	0.02	0.001	0.002	1.5%	-2.89	-0.069	-0.185
wheelcover-rear	-0.01	0.000	-0.001	-0.6%	-0.26	-0.006	-0.017
rear-lower	0.03	0.001	0.002	1.8%	-0.28	-0.007	-0.018
tail	-0.09	-0.002	-0.006	-6.0%	0.00	0.000	0.000
Miscellaneous	0.00	0.000	0.000		0.00	0.000	0.000
TOTAL	1.585	0.038	0.101	100%	-0.940	-0.022	-0.060

Table 6

	ΔCd	ΔCl
Shell-body	0.002	0.039
Shell-front	-0.002	0.004
Wheel front	0.000	0.000
Wheel rear	0.000	0.000
wheelcover-front	0.000	0.013
wheelcover-rear	0.000	-0.002
rear-lower	0.001	-0.003
tail	0.000	0.000
TOTAL	0.001	0.050

Table 7. Drag and lift differences over the PIDs and total comparing Case D to Case A

Discussion

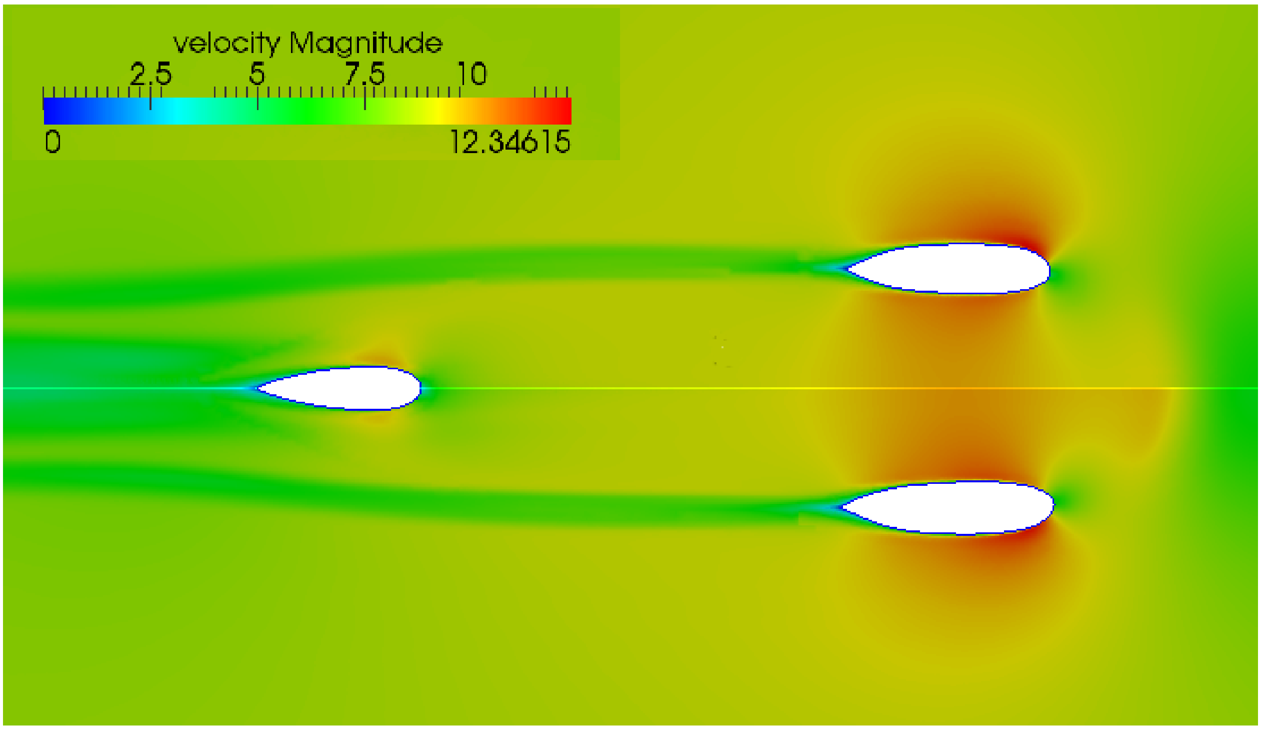

Figure 11. Flow velocity 35mm above ground for Case A(lower half) and Case C(upper half)

As shown above in Figure 11, Case D does not accelerate the flow as much as in Case A mainly because the nose is higher from the ground at the front of the vehicle. And the inclination of the underbody reduced the downforce by 50 drag counts.

Case E

Residuals

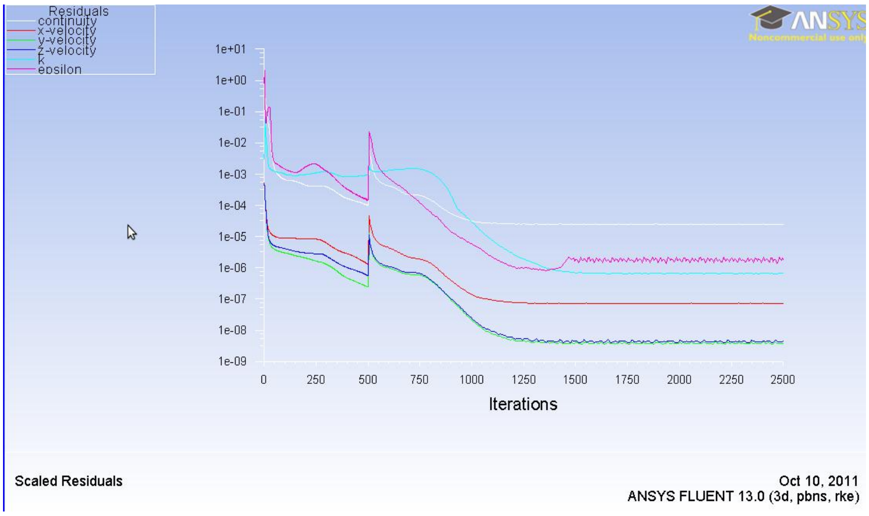

Plot 5. Residuals plot for case E

Aerodynamic forces

	Force x-dir (N)	Cd*A	Cd	%	Force z-dir (N)	Cl*A	Cl
Shell-body	-0.60	-0.014	-0.039	-49.0%	2.38	0.057	0.154
Shell-front	2.02	0.048	0.131	164.6%	-0.83	-0.020	-0.054
Wheel front	0.00	0.000	0.000	0.1%	-0.25	-0.006	-0.016
Wheel rear	0.00	0.000	0.000	-0.4%	-0.04	-0.001	-0.003
wheelcover-front	0.00	0.000	0.000	0.2%	-3.20	-0.077	-0.207
wheelcover-rear	-0.03	-0.001	-0.002	-2.8%	-0.24	-0.006	-0.016
rear-lower	0.00	0.000	0.000	0.4%	-0.28	-0.007	-0.018
tail	-0.16	-0.004	-0.010	-13.0%	0.00	0.000	0.000
Miscellaneous	0.00	0.000	0.000		0.00	0.000	0.000
TOTAL	1.230	0.029	0.080	100%	-2.470	-0.059	-0.160

Table 8. Distribution of aerodynamic forces and coefficients for Case E

	ΔCd	ΔCl
Shell-body	-0.011	-0.031
Shell-front	-0.003	-0.004
Wheel front	0.000	-0.001
Wheel rear	0.000	0.000
wheelcover-front	-0.001	-0.010
wheelcover-rear	-0.002	-0.001
rear-lower	-0.001	-0.003
tail	-0.004	0.000
TOTAL	-0.021	-0.049

Table 9. Drag and lift differences over the PIDs and total comparing Case E to Case A

Discussion

Looking at Table9, Case E which is the unrefined mesh was giving a much lower drag and a higher downforce then the refined mesh. At the beginning it was believed that this was a more accurate prediction of the drag since as seen in the zero total pressure iso-surfaces below the wake around the front wheelcover has a better resolution, is more continuous and has a smoother shape; which is to be expected since there are no strong vortices and the Vera body is relatively smooth. However the difference of 20 drag counts could be an indication that drag was being over predicted in the refined meshes.

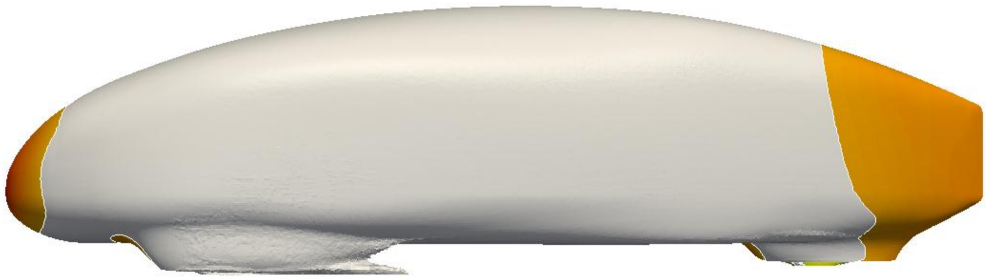

Figure 12. Zero total pressure iso-surfaces for Case A

Figure 13. Zero total pressure iso-surfaces for Case E

However the existence of an iso-surface layer covering most of the vehicle and the fact that it didn't change in all refined configurations led to investigate the reasons for that. The y_plus distribution for both case was plotted and the results are shown in Figures 14 and 15. As shown in Figure 14 the y_plus distribution over Vera is mostly below 11.6. Due to the inaccuracy of the wall treatment in fluent then fluent will solve any y_plus under 11.6 as laminar flow which might be the reason why the iso-surface covers most of the vehicle in case A. In Case E the y_plus values are mostly above 11.6 on Vera so fluent will solve them as turbulent flow. For the k-epsilon model used to solve, it is recommended that the y_plus values are between 30 and 150 or 30 and 300 according to the fluent user guide. So the results of the simulation done might be questionable due to the fact that y_plus is not within the recommended range however this issue was discovered really late in the project and there was no time to try more simulations in Ansa.

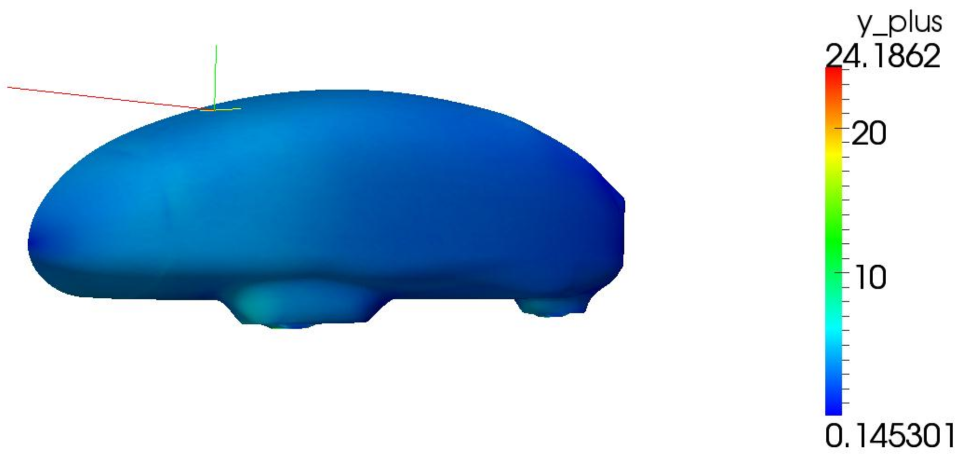

Figure 14. y_plus distribution over Vera in Case A

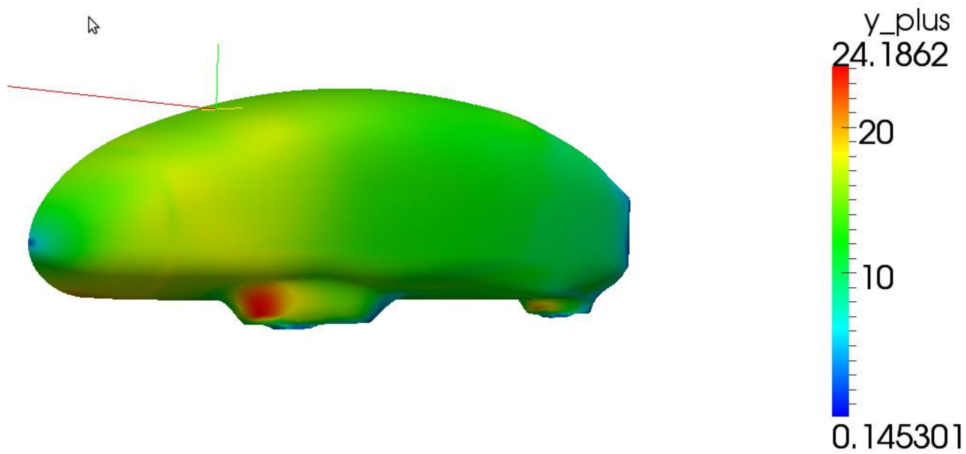

Figure 15. y_plus distribution over Vera in Case E

1st order vs. 2nd order discretization

Residuals

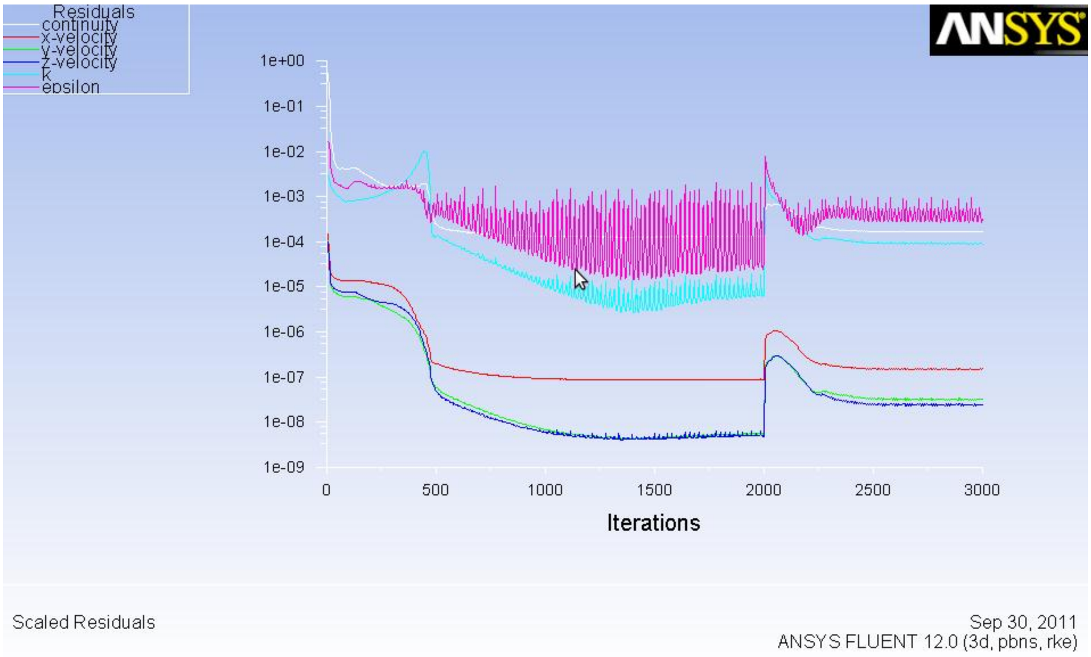

Plot 6. Residuals plot for 1st order and 2nd order discretization

Aerodynamic forces

	ΔCd	ΔCl
Shell-body	**0.005**	**0.007**
Shell-front	**0.001**	**0.000**
Wheel front	**0.000**	**-0.001**
Wheel rear	**0.000**	**0.000**
wheelcover-front	**0.000**	**-0.001**
wheelcover-rear	**0.000**	**0.000**
rear-lower	**0.000**	**0.000**
tail	**-0.001**	**0.000**
TOTAL	0.005	0.004

Table 10. Drag and lift differences over the PIDs and total comparing 2nd to 1st order discretization

Discussion

While investigating the effects of first and second order the same mesh was run up to 2000 with 1st order upwind discretization for k and epsilon and then it was switched to 2nd order for 1000 more iterations. Note that the momentum discretization was set from the beginning to 2nd order. From plot 6, it is clear that 2nd order discretization had much more stable k and epsilon residuals. Although the standard deviation of Cd and Cl were within 0 drag counts on 1st order they did change to another stable solution with the second order discretization. Since the second order discretization involves more cells and hence gives more accurate results then all final solutions where represented in second order.

Simple vs. Couple solving schemes

Residuals

Plot 7. Residuals plot for simple to couple solving schemes

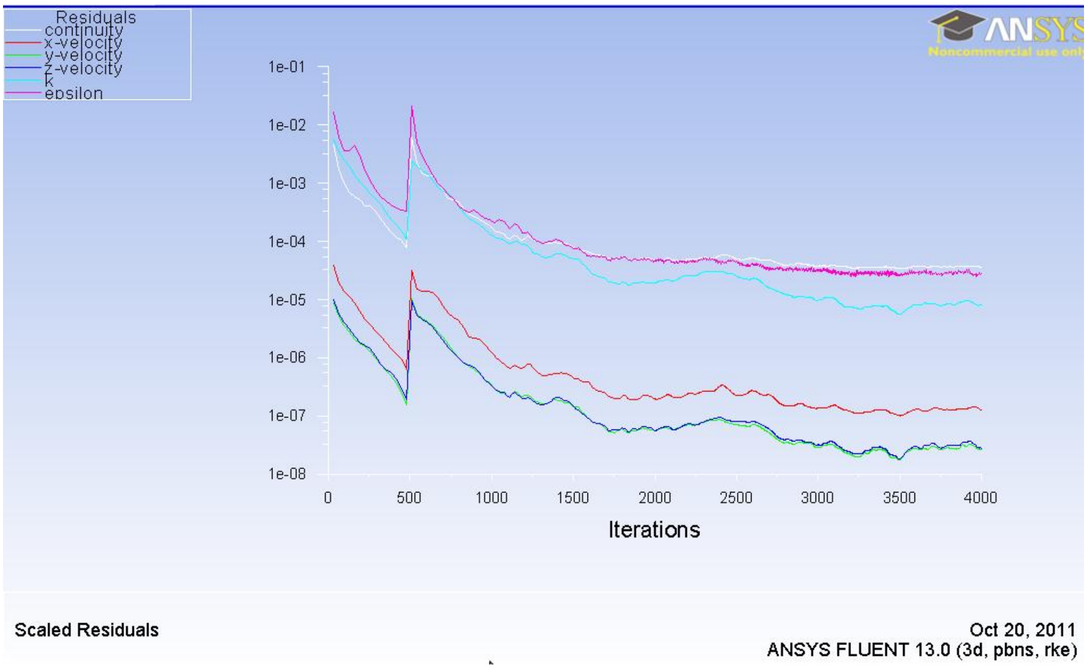

Plot 8. Residuals plot for couple solving scheme

Aerodynamic forces

No analysis of the force distribution on the different PIDs was done, however in total the drag converged to the same value however the lift was 5 counts higher.

Discussion

In plot 7 one can see the difference between solving the first 3500 iterations with a simple solving scheme and then it was switched to couple solving scheme where the under-relaxation factors for pressure and momentum where 0.3 until 4500 and then they were decreased to 0.2 for 1000 more iterations. The results show that the solution converges for both simple and couple however running from couple from the start gave slightly different results which are expected to be more accurate since Fluent is solving the pressure and momentum equations simultaneously in coupled mode while it solves them separately in the simple scheme. One can also notice that the convergence in the couple was higher and it gave more stable residuals.

Conclusions

Many conclusions can be drawn from the cases above however some of them might not be completely accurate since all CFD results are mesh and solving settings dependent. Below are some conclusions that were made taking those settings changes and their effects into consideration:

- For more accurate results and faster convergence, if using the k-epsilon model then the couple solving scheme should be used from the start with 2nd order discretization for momentum, epsilon and k.
- An investigation should be done on different turbulence models since they might be more suitable then the k-epsilon in solving boundary layers at the surface.
- Take care of the y_plus values and always check that you are within the recommended range of the turbulence model you are using.
- 2000 iterations are usually enough for convergence.
- A more thorough investigation should be carried out to identify the laminar spots on Vera since it has a smooth shape and is running at low velocities.
- The most effective way of controlling lift/downforce is to change the design of the wheel covers to control air velocity in between the wheel covers.

Vera 2

As stated in the aim, from the knowledge gained from the work done on Vera and analyzing the results, the next step is to implement and design Vera 2. At the moment, the first version of Vera 2 is completed. The first version of Vera 2 can be seen in figure XX. The total length is increased, with a small nose area where the total frontal area decreased with about 30 %. The drag coefficient between Vera and Vera 2 is quite similar when comparing he results, however sense the fontal area is smaller, which is what matters when comparing, the drag is reduced. The wheel covers is also important factor with significant effect on lift. On Vera 2 they have a smaller frontal area and are slightly longer. On the first version of Vera 2, to different configurations of the wheel covers are simulated, one that is symmetric and one that is cambered. On figure XX the differences can be seen. The cambered wheel cover forces the flow around on the outside of the vehicle giving a high pressure region under that vehicle sense the flow decelerates. However the symmetric wheel cover distributes the flow both on the inside and outside of the Vehicle. This causes a venturi effect around the wheel covers under the vehicle with a low pressure region where the flow accelerates. As seen in the figure, the lift transferred to down force when the wheel covers changes form cambered to symmetric.

The work on Vera 2 will continue by simulating different configurations on the problematic areas, analyzing the results and completing a final version of Vera 2.

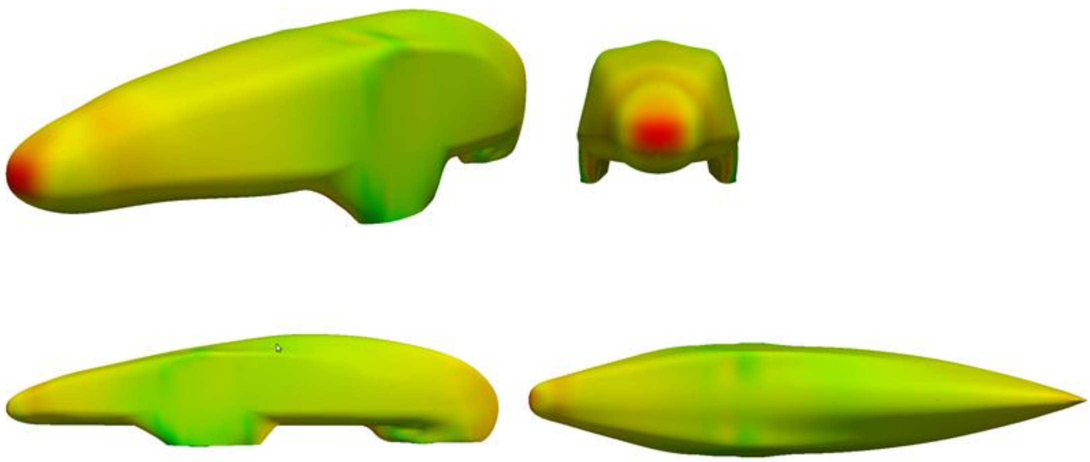

Figure 16 Vera 2 version 1

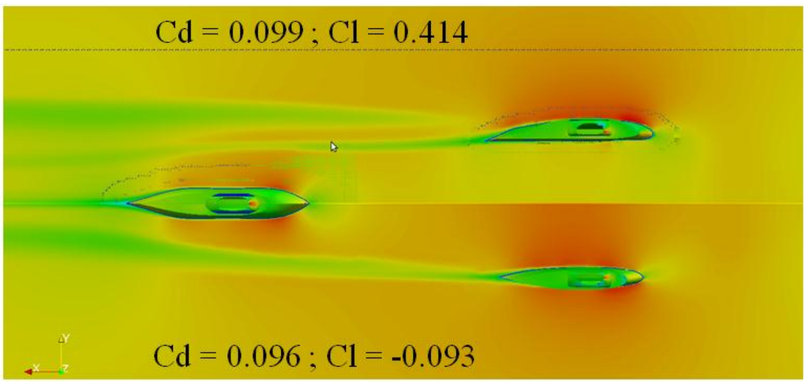

Figure 17 Cambered vs. Symmetric wheel cover

References

Literature:

Road Vehicle Aerodynamics Advanced Course – CFD GUIDELINES

R H Bernard. 2010. Road Vehicle Aerodynamics Design, Mechaero Publishing, Great Britain, 9780954073473

Tutorials:

External Aero – Ansa Meshing

Papers:

Pope, Stephen B. 2000. *Turbulent Flows.* Cambridge : Cambridge University Press, 2000. 978-0-521-59886-6

Hägerström, Fredrik. 2010. *Prediction of Cooling Drag using CFD*: Lund University, 2010. ISSN 0282-1990